Lab on a Chip

Cite this: *Lab Chip*, 2012, **12**, 3866–3869

www.rsc.org/loc

TECHNICAL INNOVATION

"Overpass" at the junction of a crossed microchannel: An enabler for 3D microfluidic chips†‡

Yan He,[a] Bai-Ling Huang,[a] Dong-Xiao Lu,[b] Jia Zhao,[b] Bin-Bin Xu,[a] Ran Zhang,[a] Xiao-Feng Lin,[a] Qi-Dai Chen,[a] Juan Wang,[a] Yong-Lai Zhang*[a] and Hong-Bo Sun*[ab]

Received 24th April 2012, Accepted 11th July 2012
DOI: 10.1039/c2lc40401j

Reported here is the design and fabrication of three-dimensional (3D) "overpass" microstructures at the junction of crossed microfluidic channels by femtosecond laser direct writing of photopolymers. The post-integrated overpass could be used for guiding different microfluids across the junction without mixing; therefore it is proposed as an enabler for achieving 3D microfluidic chips based on conventional two-dimensional (2D) microchannels. As representative examples, bi-crossed and tri-crossed microchannels have been equipped with bi-connected and tri-connected overpasses, respectively. Flow tests confirm 3D flowing capability. The integration of such overpass structures at the microchannel junction provides an opportunity to impart 3D capability to conventional 2D microchips, thus the method may hold great promise for both functionalization and miniaturization of Lab-on-a-Chip systems.

Introduction

Over the past two decades, the micrototal analysis system (μTAS), represented by Lab-on-a-Chip (LoC), has undergone thorough developments due to its distinct advantages of low consumption, high sensitivity, safety and environmental friendliness.[1–4] To date, despite a short history, LoC systems have already revealed a broad range of potential applications concerning multidisciplinary research fields.[5–11] However, the commonly used microfluidic devices are generally based on two-dimensional (2D) microchannels,[12] which could be readily fabricated by standard photolithography, soft lithography technique and other novel techniques.[13] In recent years, with the increasing complexity of microfluidic systems, there is a growing need to develop three-dimensional (3D) microchannels,[14–19] allowing for more complex functionalities such as 3D cell patterning,[15] solutions mixing,[20] light manipulation,[21] and even solving hard problems computationally.[16] Triggered by the promising properties derived from 3D structures, up to now, there already exist a series of successful examples of 3D microchannels. For instance, 3D microchannel could be readily fabricated by femtosecond laser microprocessing of photosensitive glass[22] or two-photon microfabrication of positive tone photoresists.[23] Additionally, Whitesides and co-workers have developed an ingenious methodology for the preparation of various 3D polydimethylsiloxane (PDMS) microchannels through divers schemes such as mechanical deformation of straight channels,[17] "solid-object printing"[18] and "membrane sandwich" methods.[19] Later, 3D PDMS chips have also been prepared by using "perforated membrane" method,[24] and "surface treated" PDMS as transferring layers.[25] Generally, the basic principle for the fabrication of these 3D PDMS microchannels is the precise assembly and ordered stacking of 2D patterned PDMS layers. The whole process should be carried out with special care, somewhat depending on the craft work, and the procedure is usually of considerable complexity. Moreover, the application of those 3D microchannels would suffer from serious problems when they are integrated with other 2D microchips. So an ingenious route to rational design, fabrication and integration of 3D microchannels is still highly desired. Perhaps to endow those commonly used 2D microchannels with 3D capability could be an alternative approach to reach this end, but obviously, it remains a technical challenge.

On the other hand, with the rapid development of LoC systems, microfluidic chip designs are being designed with greater complexity, miniaturization and high integration. Since conventional 2D microfluidic chips do not allow two microchannels to cross without connecting, different microchannels have to be arranged circuitously, which not only increases the whole chip size, but also debases the sensitivity and efficiency of

[a]*State Key Laboratory on Integrated Optoelectronics, College of Electronic Science and Engineering, Jilin University, 2699 Qianjin Street, Changchun, 130012, People's Republic of China. E-mail: yonglaizhang@jlu.edu.cn; Fax: +86-431-85168281; Tel: +86-431-85168281*
[b]*College of Physics, Jilin University, 119 Jiefang Road, Changchun, 130023, People's Republic of China. E-mail: hbsun@jlu.edu.cn*

† Electronic Supplementary Information (ESI) available: Experimental section; fluorescence microscopic image of the flow test of R6G and coumarin solutions; optical image of the overpass structure during stability tests; contours of velocity of microfluid inside a microchannel and SEM image of overpass structure fabricated inside a SU-8 microchannel. See DOI: 10.1039/c2lc40401j

‡ Published as part of a themed issue dedicated to Emerging Investigators

the LoC system due to the large channel length. In this case, to make the crossed channel passable but unconnected is critical to overcome this limitation.

Inspired from the overpasses that were constructed to regulate the traffic, we report here the design and fabrication of a micro-overpass structure at the junction of crossed microchannels, which could be used to endow conventional 2D microchannels with 3D capability and therefore act as a traffic-control device to guide the microfluids across the junction without mixing. Recently, a two photon photopolymerization (TPP) technique has been proved a powerful tool for 3D micronanofabrication,[26] revealing great potential for chip functionalization.[27–32] In our work, we fabricate the 3D overpass structure inside a microchannel by femtosecond laser direct writing (FLDW) of photopolymers. Flow tests confirm that, with the help of post integrated overpass structures, the 2D microchannels show 3D flow property. The unique overpass structure at the junction of the 2D microchannels would be considered as an enabler to 3D microfluidic chips.

Results and discussion

The fabrication of overpass microstructures was carried out on conventional glass-based microchips prepared by classical wet-etching method (for details of the experiments, see ESI†). Typically, bi- and tri-crossed microchannels have been used for the FLDW fabrication. Shown in Fig. 1 is the schematic illustration of the FLDW processing system and our basic concept. A femtosecond laser with 80 MHz repetition rate, 120 fs pulse width and 800 nm central wavelength was focused by a 60× oil immersion objective lens to direct write on the junction of the microchannel. During the fabrication, the entire process including the focusing of laser beam and the positioning of sites to be addressed was monitored by the Charge Coupled Device (CCD) set. The laser scanning path was precisely controlled by computer according to the preprogrammed structures from the bottom slice to the upside slice until the entire 3D structure is

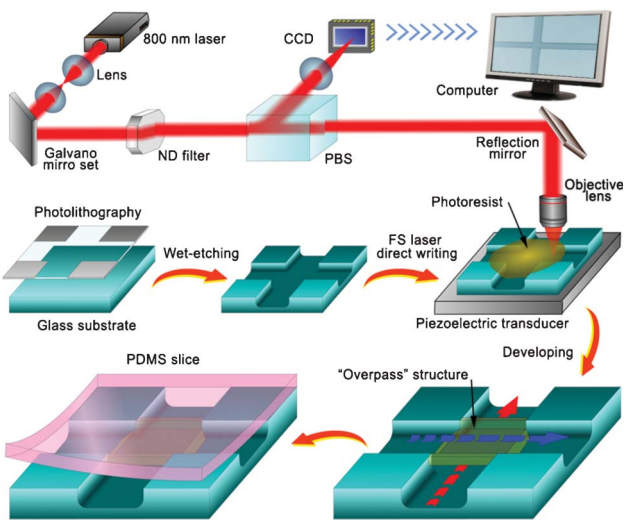

Fig. 1 Schematic illustration for the FLDW fabrication of polymeric 3D overpass structure at the junction of a glass-based microfluidic channel prepared by wet etching.

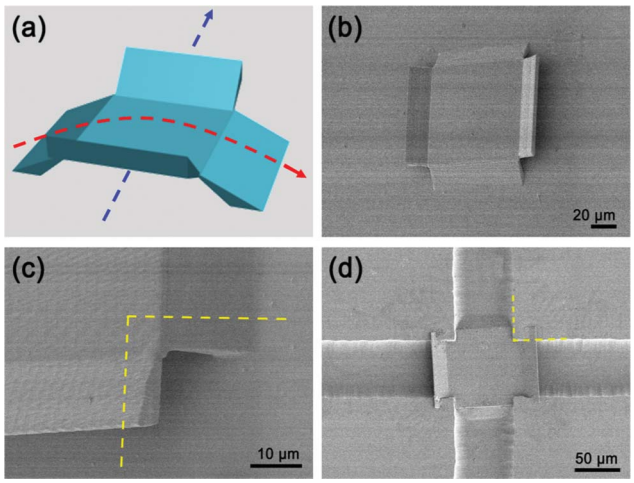

Fig. 2 (a) 3D model of the overpass structure for the two-channel crossed junction; (b) SEM image of the bi-connection overpass structure fabricated on planar substrate; (c) SEM image of the magnified detail of the overpass structure. The yellow lines indicate the edge of crossed microchannel; (d) SEM image of an overpass fabricated at the junction of a crossed microchannel, which is used for 3D chips.

achieved. After the FLDW fabrication, the microchannel, together with the SU-8 microstructure, was rinsed in SU-8 developer. In this procedure, unpolymerized resins were removed and the 3D overpass structure has been embellished at the junction of the crossed microchannel.

Fig. 2a shows the 3D model of the overpass structure designed for the bi-crossed microchannel. The overpass structure is constituted by two layers which allows different microfluids to pass through, and two couples of protecting walls for preventing leakage. Despite the fact that the structure is very simple, the fabrication of such a 3D microstructure seems impossible for conventional lithography technique. However, by taking advantage of the powerful 3D processing capability of two-photon photopolymerization, the designed structure could be readily fabricated. Fig. 2b is a SEM image of the fabricated overpass structure. It could be clearly identified that the surface of the overpass structure is very smooth, indicating the high quality of the femtosecond laser direct writing. The thickness of the polymer layer is about 2 μm; and the size of the protection walls of the overpass is measured to be ~80 μm, which is larger than that of our microchannel (~60 μm). The larger design size is to guarantee a better seal and prevent undesired leakage. As shown in Fig. 2c, the yellow line indicates the edge of the microfluidic channel. When the overpass structure was fabricated at the junction of the microfluidic channel, the superfluous region embedded into the glass could not be fabricated. The excessive laser scanning region is very important for a seamless connection between polymer structure and the glass microchannel walls. Fig. 2d shows the SEM image of an overpass structure fabricated at the junction of a bi-crossed microfluidic channel. It was found that, in such an overpass-integrated microchannel, microfluids in the horizontal channel would pass through the junction bellow the bridge, whereas the microfluids in the vertical channel would flow above.

The performance of our overpass was evaluated by using two kinds of aqueous solutions with different colors. As shown in

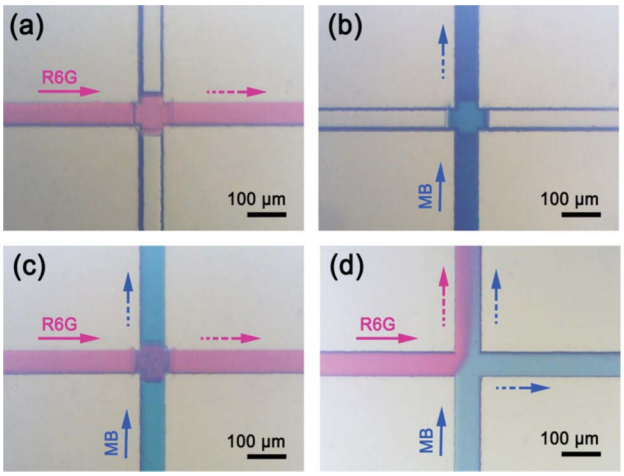

Fig. 3 Optical microscopic images of the flow tests. (a) The aqueous solution of R6G flows through the overpass in the horizontal channel; (b) The aqueous solution of MB flows through the overpass in the vertical channel; (c) The aqueous solutions of R6G and MB flow through the overpass synchronously in different channels. (d) Control experiment of the flow test in a crossed microchannel without overpass structure. The mix of two solutions was observed. The arrows indicate the flow direction.

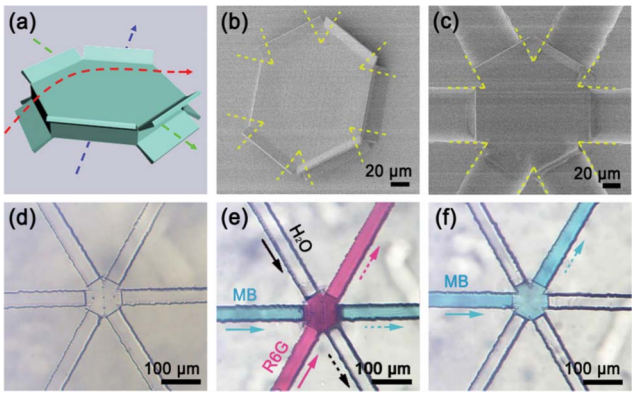

Fig. 4 (a) 3D model of the overpass structure for the three-channel crossed junction; (b) SEM image of the tri-connection overpass structure fabricated on planar substrate. The yellow lines indicate the edges of crossed microchannel; (c) SEM image of a tri-connection overpass fabricated at the junction of a tri-crossed microchannel. The yellow lines mark the edge of the crossed microchannels; (d) Optical microscopic image of the tri-crossed microchannel with tri-connection overpass; (e) The aqueous solutions of R6G and MB, as well as water flow through the overpass synchronously in different channels. (f) The aqueous solution of MB flows through the overpass and changes its flow direction. The arrow indicates the flow direction.

Fig. 3a, after covering the microchannel with a PDMS slice, the solution of Rhodamine 6G (R6G), represented by the pink color, was injected into the horizontal channel at the speed of 5 mL h^{-1} first. It could be clearly observed form the image that, the R6G solution passes through the overpass without any leakage. Then a blue methylene blue trihydrate (MB) solution was injected into the vertical channel at the same speed (5 mL h^{-1}), it also passes through the overpass freely, indicating the interconnectivity of our overpass in both horizontal and vertical direction (Fig. 3b). When we synchronously injected the two kinds of solutions into the crossed microchannel, it could be observed that the two fluids pass across the junction without mixing, indicating the 3D flowing property. In order to check whether there is a leak, fluorescent solutions of R6G and coumarin were also used for the test; and the fluorescence microscopic image confirms that there have been no leakages (Fig. S1, ESI†). For comparison, a control experiment was carried out. As shown in Fig. 3d, when R6G and MB solutions were injected into a crossed microchannel without the overpass, a clear mixing was observed.

Beside the interconnectivity tests, the stability of the overpass structure was also taken into account. Fig. S2, ESI†, shows the optical microscopic images of the flow tests at 50, 70, and 90 °C, as well as for a long time (1d, 7d). Notably, no leakage of the pink R6G solution could be identified, indicating the excellent thermal stability and durability of the system. It is worth noting that, as the microchannel was divided into two layers, the overpass structure would show certain influence on the flow property. For example, the velocity of the fluids may double under the overpass, the square corner may shows resistance to the fluids, especially at high flow rate. In this regards, the trapeziform design of overpass profile can significantly reduce the flow resistance, as shown in Fig. S3, ESI†.

The concept of constructing an overpass at the microchannel junction is not limited to bi-crossed microfluidic channel, for other complex junctions, the method is also workable. In fact, the pass through performance mainly depends on the structural design according to the geometric pattern of the microchannels. We present here another example of overpass structure based on a tri-crossed microchannel. Shown in Fig. 4a is the 3D model of the tri-connected overpass. In this case, the overpass is designed as a hexagon according to the shape of the tri-connected junction. There exist three layers for the whole overpass. In each layer, there is one entrance and one exit that allow microfluids to pass through, and four protecting walls to prevent leakage. It is worthy pointing out that the assignment of the entrance and exit is flexible in the design principle, so you can control the flowing direction of microfluids in each channel by design and fabrication of different overpass structures.

In the present model, different microfluids could pass straight through the junction without mixing. Fig. 4b shows the SEM image of the tri-connected overpass structure fabricated on glass substrate according to this prototype. The basic shape is a hexagon with the edge length of ~80 μm, which is lager than the channel width of ~60 μm (see the yellow lines). As mentioned previously, the larger size in width is to ensure a tight connection to the channel. Fig. 4c shows the SEM image of the overpass structure fabricated at the junction of a tri-connected microchannel. Obviously, the overpass structure was well integrated at the microchannel junction. Note that the total length of the overpass is larger than 100 μm, so in order to stablish the layer structure, five columniform piers have been added in the center of the overpass at the bottom two layers during the laser fabricating. The piers could be easily identified from the optical microscopic image (Fig. 4d).

In the test of flowing connectivity, R6G and MB aqueous solutions as well as pure water was injected in to different microfluidic channels at the same time. The arrows in Fig. 4e indicate the flow direction of different microfluids. The distinct

colors in different channels indicate that divers microfluids could pass across the junction through the overpass separately. In addition to the straight overpass, as a representative illustration, we also design and fabricate a direction-changed overpass. As shown in Fig. 4f, MB was injected into the horizontal channel, whereas after passing through the overpass, it changed its direction and flows into another channel. In fact, the design principle is very flexible, both the entrance and exit in each layer could be assigned arbitrarily according to different requirements. Besides, the use of SU-8 series photoresist is not indispensable, other negative tone photoresist such as methacrylate-based photopolymers and Norland Optical Adhesive (NOA) series photoresist could also be adopted for this fabrication. Nevertheless, the compatibility between the photopolymer, developer and the channel material should be taken into account. In addition to the glass-based microchannel, various polymer-based microchannels made from PMMA, PS and PDMS could also be used for the integration of overpass structures. However, due to the use of strong organic solvents (*e.g.*, acetone) in the developing process, a highly cross-linked polymer network or passivated surface of the microchannel is necessary. Considering the homogeneous surface property, the microchannel made from SU-8 photoresist would be a preferred choice. In this case, the microchannel and overpass structure could be fabricated by photolithography and FLDW in sequence, as shown in Fig. S4 ESI†.

Conclusions

Inspired from various overpasses used for regulating the traffic, 3D overpass structures have been designed and fabricated successfully at the junction of microfluidic channels by using FLDW of photopolymers. The designability and 3D processing capability make the FLDW a powerful tool for on-chip construction of desired 3D structures. Both bi- and tri-crossed microchannels have been chosen as typical candidates for the embellishment of bi- and tri-connected overpasses, respectively. In the flow tests, the post integrated overpass guide the microfluids pass across the micro-channel junction without mixing. Additionally, the flow properties in different microchannels, including flow direction, interflowing and distribution, could be flexibly designed and fabricated according requirement. The integration of the overpass endows the 2D microchannel with 3D flowing capability, and thus it could be considered as an enabler for fabricating 3D microchannels based on conventional 2D microchips. This novel technique may find broad application in functionalization and miniaturization of Lab-on-a-Chip systems.

Acknowledgements

This work is supported by the National Science Foundation of China (Grant Nos. 61008014, 90923037 and 6078048). We also acknowledge the China Postdoctoral Science Foundation No. 20110490156 and the Hong Kong Scholar Program XJ2011014.

References

1 H. Craighead, *Nature*, 2006, **442**, 387–393.
2 R. Daw and J. Finkelstein, *Nature*, 2006, **442**, 367–367.
3 W. Y. Lin, Y. J. Wang, S. T. Wang and H. R. Tseng, *Nano Today*, 2009, **4**, 470–481.
4 G. Velve-Casquillas, M. Le Berre, M. Piel and P. T. Tran, *Nano Today*, 2010, **5**, 28–47.
5 I. Barbulovic-Nad, S. H. Au and A. R. Wheeler, *Lab Chip*, 2010, **10**, 1536–1542.
6 S. L. S. Freire and A. R. Wheeler, *Lab Chip*, 2006, **6**, 1415–1423.
7 M. He and A. E. Herr, *J. Am. Chem. Soc.*, 2010, **132**, 2512–2513.
8 S. Tia and A. E. Herr, *Lab Chip*, 2009, **9**, 2524–2536.
9 E. W. K. Young, M. W. L. Watson, S. Srigunapalan, A. R. Wheeler and C. A. Simmons, *Anal. Chem.*, 2010, **82**, 808–816.
10 B. B. Xu, Z. C. Ma, H. Wang, X. Q. Liu, Y. L. Zhang, X. L. Zhang, R. Zhang, H. B. Jiang and H. B. Sun, *Electrophoresis*, 2011, **32**, 3378–3384.
11 D. P. Wu, J. H. Qin and B. C. Lin, *J. Chromatogr., A*, 2008, **1184**, 542–559.
12 Z. Y. Li, K. Sun, M. Sunayama, R. Araki, K. Ueno, M. Abe and H. Misawa, *Electrophoresis*, 2011, **32**, 3392–3398.
13 Y. Lu, B. C. Lin and J. H. Qin, *Anal. Chem.*, 2011, **83**, 1830–1835.
14 X. Q. Gong, X. Yi, K. Xiao, S. Li, R. Kodzius, J. H. Qin and W. J. Wen, *Lab Chip*, 2010, **10**, 2622–2627.
15 D. T. Chiu, N. L. Jeon, S. Huang, R. S. Kane, C. J. Wargo, I. S. Choi, D. E. Ingber and G. M. Whitesides, *Proc. Natl. Acad. Sci. U. S. A.*, 2000, **97**, 2408–2413.
16 D. T. Chiu, E. Pezzoli, H. K. Wu, A. D. Stroock and G. M. Whitesides, *Proc. Natl. Acad. Sci. U. S. A.*, 2001, **98**, 2961–2966.
17 H. K. Wu, T. W. Odom, D. T. Chiu and G. M. Whitesides, *J. Am. Chem. Soc.*, 2003, **125**, 554–559.
18 J. C. McDonald, M. L. Chabinyc, S. J. Metallo, J. R. Anderson, A. D. Stroock and G. M. Whitesides, *Anal. Chem.*, 2002, **74**, 1537–1545.
19 J. R. Anderson, D. T. Chiu, R. J. Jackman, O. Cherniavskaya, J. C. McDonald, H. K. Wu, S. H. Whitesides and G. M. Whitesides, *Anal. Chem.*, 2000, **72**, 3158–3164.
20 D. Therriault, S. R. White and J. A. Lewis, *Nat. Mater.*, 2003, **2**, 265–271.
21 O. J. A. Schueller, X. M. Zhao, G. M. Whitesides, S. P. Smith and M. Prentiss, *Adv. Mater.*, 1999, **11**, 37–41.
22 Y. Liao, J. X. Song, E. Li, Y. Luo, Y. L. Shen, D. P. Chen, Y. Cheng, Z. Z. Xu, K. Sugioka and K. Midorikawa, *Lab Chip*, 2012, **12**, 746–749.
23 W. H. Zhou, S. M. Kuebler, K. L. Braun, T. Y. Yu, J. K. Cammack, C. K. Ober, J. W. Perry and S. R. Marder, *Science*, 2002, **296**, 1106–1109.
24 Y. Q. Luo and R. N. Zare, *Lab Chip*, 2008, **8**, 1688–1694.
25 M. Y. Zhang, J. B. Wu, L. M. Wang, K. Xiao and W. J. Wen, *Lab Chip*, 2010, **10**, 1199–1203.
26 Y. L. Zhang, Q. D. Chen, H. Xia and H. B. Sun, *Nano Today*, 2010, **5**, 435–448.
27 T. W. Lim, Y. Son, Y. J. Jeong, D. Y. Yang, H. J. Kong, K. S. Lee and D. P. Kim, *Lab Chip*, 2011, **11**, 100–103.
28 Y. Tian, Y. L. Zhang, J. F. Ku, Y. He, B. B. Xu, Q. D. Chen, H. Xia and H. B. Sun, *Lab Chip*, 2010, **10**, 2902–2905.
29 J. Wang, Y. He, H. Xia, L. G. Niu, R. Zhang, Q. D. Chen, Y. L. Zhang, Y. F. Li, S. J. Zeng, J. H. Qin, B. C. Lin and H. B. Sun, *Lab Chip*, 2010, **10**, 1993–1996.
30 D. Wu, Q. D. Chen, L. G. Niu, J. N. Wang, J. Wang, R. Wang, H. Xia and H. B. Sun, *Lab Chip*, 2009, **9**, 2391–2394.
31 B. B. Xu, H. Xia, L. G. Niu, Y. L. Zhang, K. Sun, Q. D. Chen, Y. Xu, Z. Q. Lv, Z. H. Li, H. Misawa and H. B. Sun, *Small*, 2010, **6**, 1762–1766.
32 B. B. Xu, R. Zhang, X. Q. Liu, H. Wang, Y. L. Zhang, H. B. Jiang, L. Wang, Z. C. Ma, J. F. Ku, F. S. Xiao and H. B. Sun, *Chem. Commun.*, 2012, **48**, 1680–1682.